The Asymptotic Structure of the Hodgkin-Huxley Equations

Rebecca Suckley[1] and Vadim N. Biktashev[1,2,*]

November 21, 2002

[1] *Department of Mathematical Sciences, University of Liverpool, Liverpool L69 7ZL, UK*
[2] *On leave from: Institute for Mathematical Problems in Biology, Pushchino, 142290, Russia*
[*] *Author to whom correspondence should be addressed.*

Abstract

We analyse the asymptotic structure of the Hodgkin-Huxley system of equations, in terms of the concepts of slow manifold and fast foliation, based on Tikhonov's theorem on asymptotics of solutions of slow-fast systems of differential equations. We test Zeeman's conjecture that the jump onset - slow return structure of the action potential in realistic equations of biological excitability may be due to a cusp singularity of the slow manifold with respect to the fast foliation. We find that although the cusp singularity can appear in such equations, the characteristic features in question cannot be reproduced within the Tikhonov scheme and require development of different asymptotic approaches.

1 Introduction

Fifty years ago, Hodgkin & Huxley (1952) suggested a system of differential equations describing the flow of electric current through a surface membrane of a giant nerve fibre. Later this system of equations became a prototype of a large family of mathematical models quantitatively describing electrophysiology of various living cells and tissues. In this paper, we study the mathematical properties of the Hodgkin-Huxley (HH) system of equations, using methods of singular perturbation theory in the sense of Tikhonov (1952) theorem.

The idea of the present study came from a 1972 paper by Zeeman (Zeeman 1972),(Zeeman 1977, pp.81–140). In that paper, Zeeman considered equations of biological excitability as singularly perturbed systems, and introduced the concepts of the slow manifold and fast foliation for their formal analysis. This analysis has led him to a conjecture that certain features of the solutions of the biological equations, specifically, slow return from the excited state as opposed to its jump onset, can be explained by a cusp catastrophe in the projection of the slow manifold along the fast foliation.

Understanding asymptotic structure of equations is important for practical applications, as it allows development of adequate approximate procedures that save computation time, and provide intuitive insight, which is not possible in detailed, exact models. Partial differential equations of the reaction diffusion type, that describe propagation of excitation in cardiac tissue, have in their reaction part models of excitability that are, historically and mathematically, descendants of the Hodgkin-Huxley system. There is a well-developed asymptotic theory that describes propagation of waves in such systems (Tyson & Keener 1988). However, that theory depends on the assumption of the action potential having both jump onset of excitation and jump return from it, and so is not applicable to systems with smooth return. This makes its applicability to biological systems of Hodgkin-Huxley type questionable. It has been found recently, that the jump onset-jump return assumption significantly limits the variety of possible qualitative behaviours of the excitation waves, particularly for description of re-entrant arrhythmias in the heart (Elkin, Biktashev & Holden 2002).

In recent years, there were several attempts to analyse and simplify realistic excitability equations, based on different ideas and pursuing different applications, see e.g. (Fenton & Karma 1998,

Duckett & Barkley 2000, Bernus, Wilders, Zemlin, Verschelde & Panfilov 2002, Hinch 2002). In this paper, we apply Zeeman's analysis to the Hodgkin-Huxley system of equations, to study the geometry of its slow manifold and fast foliation, and in particular, to test Zeeman's conjecture on the role of the cusp catastrophe. We do this for a family of systems, obtained from the original Hodgkin-Huxley system by variation of one of its parameters, the reversal potential of the leakage current. The result is that Zeeman's conjecture is partly true: the slow manifold in the considered family of systems can have a cusp catastrophe; however, this does not explain the feature of the action potential mentioned above. We conclude from these results that whereas Zeeman's conjecture in its original form may be true for some biological excitability equations, explanation of the action potential shape in other models, including the HH system, may require more sophisticated asymptotic approaches than that suggested by Tikhonov and Zeeman.

The structure of this paper is as follows. In Section 2 we introduce the Hodgkin-Huxley system of equations, which is the object of the present study. In Section 3 we present Tikhonov's theorem, as the formal basis for the asymptotic technique that is the main tool of the present study, and introduces the concepts of fast foliation and slow manifold. Section 4 describes Zeeman's speculative examples based on that technique, which motivated the present study. The main results are presented in Section 5, where we formally introduce the notion of asymptotic embedding, which allows application of the asymptotic procedure to the Hodgkin-Huxley system of equations, and Sections 6 and 7 where we apply this asymptotic procedure in two different ways. The obtained results are summarised and discussed in Section 8.

2 The Hodgkin-Huxley system of equations

$$\begin{aligned}
\frac{\mathrm{d}E}{\mathrm{d}t} &= -C_M^{-1}\left(\overline{g}_K n^4(E-E_K)+\overline{g}_{Na}m^3h(E-E_{Na})+\overline{g}_l(E-E_l)\right),\\
\frac{\mathrm{d}n}{\mathrm{d}t} &= \frac{(\overline{n}-n)}{\tau_n}=\alpha_n(1-n)-\beta_n n,\\
\frac{\mathrm{d}m}{\mathrm{d}t} &= \frac{(\overline{m}-m)}{\tau_m}=\alpha_m(1-m)-\beta_m m,\\
\frac{\mathrm{d}h}{\mathrm{d}t} &= \frac{(\overline{h}-h)}{\tau_h}=\alpha_h(1-h)-\beta_h h,
\end{aligned} \tag{1}$$

where time t is measured in ms, E is departure of the transmembrane voltage from the resting state measured in mV, E_k, $k=Na,K,l$ are the reversal potentials of sodium, potassium and leakage currents respectively, measured in the same scale as E, $\overline{g}_k$ are corresponding maximal specific conductances in $\mathrm{mS/cm^2}$, n, m, h are dimensionless "gating" variables, C_M is the specific membrane capacitance in $\mu\mathrm{F/cm^2}$, α_j, β_j, $j=h,m,n$, are gates opening and closing rates in $\mathrm{ms^{-1}}$, depending on E, $\overline{j}$ are the gates instant equilibrium values depending on E, and τ_j are the gates dynamics time scales in ms, also depending on E. The standard values of parameters and forms of the functions used in (Hodgkin & Huxley 1952) are

$$\begin{aligned}
&C_M=1,\quad \overline{j}=\alpha_j/(\alpha_j+\beta_j),\quad \tau_j=1/(\alpha_j+\beta_j)\quad (j=n,m,h),\\
&\alpha_h=0.07e^{\frac{-E}{20}},\quad \alpha_m=\frac{0.1(-E+25)}{e^{\frac{-E+25}{10}}-1},\quad \alpha_n=\frac{0.01(-E+10)}{e^{\frac{-E+10}{10}}-1},\\
&\beta_h=\frac{1}{e^{\frac{-E+30}{10}}+1},\quad \beta_m=4e^{\frac{-E}{18}},\quad \beta_n=0.125e^{\frac{-E}{80}},\\
&\overline{g}_K=36,\quad \overline{g}_{Na}=120,\quad \overline{g}_l=0.3,\\
&E_K=-12,\quad E_{Na}=115,\quad E_l=10.613.
\end{aligned} \tag{2}$$

Note the precision with which the value of E_l is specified. This was not a result of measurement, but rather a value that made $E=0$ a stationary point of the equations. The stationary point at $E=0$ was in fact postulated, as E was not the true transmembrane voltage, but rather the

deviation of the transmembrane voltage from its resting value. Thus, rather than being the most reliable parameter, E_l is the least reliable, obtained by inference rather than direct observation.

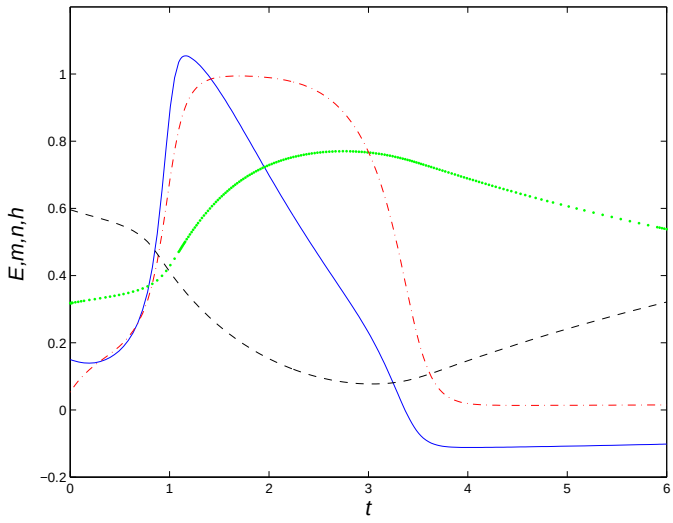

Figure 1: The action potential: transmembrane voltage E as a function of time (the blue solid line), and the gating variables as functions of time (h, black dashed line, m, red dash-dotted line, n, green dotted line), corresponding to initial conditions $E = 15$, $n = 0.3177$, $m = 0.0530$, $h = 0.5961$ in (1,2).

3 Tikhonov's singular perturbation theory

We consider a system of $k_1 + k_2$ first-order autonomous ordinary differential equations for $k_1 + k_2$ dynamic variables, of which k_1 are "slow" and k_2 are "fast". We denote the vector of slow variables $x_1 \in \mathbb{R}^{k_1}$ and the vector of fast variables $x_2 \in \mathbb{R}^{k_2}$. Then the system of equations is

$$\frac{\mathrm{d}x_1}{\mathrm{d}t} = f_1(x_1, x_2), \tag{3}$$

$$\epsilon\frac{\mathrm{d}x_2}{\mathrm{d}t} = f_2(x_1, x_2). \tag{4}$$

where $\epsilon > 0$ is a small parameter. The transformation of time $t = \epsilon T$ brings this system to the form

$$\frac{\mathrm{d}x_1}{\mathrm{d}T} = \epsilon f_1(x_1, x_2), \tag{5}$$

$$\frac{\mathrm{d}x_2}{\mathrm{d}T} = f_2(x_1, x_2). \tag{6}$$

Systems (3,4) (the slow-time system) and (5,6) (the fast-time system) are equivalent to each other for finite ϵ, but have different properties in the limit $\epsilon \to +0$.

The fast-time system at $\epsilon = 0$ becomes

$$\frac{\mathrm{d}x_1}{\mathrm{d}T} = 0, \tag{7}$$

$$\frac{\mathrm{d}x_2}{\mathrm{d}T} = f_2(x_1, x_2), \tag{8}$$

which means that the slow variables x_1 remain constant, and only the fast variables x_2 vary. A condition $x_1 = x_1^0$ for a constant x_1^0 defines a k_2-dimensional manifold $\{(x_1^0, x_2) | x_2 \in \mathbb{R}^{k_2}\}$ in the

phase space of the system $\{(x_1, x_2)\} = \mathbb{R}^{k_1+k_2}$. All such manifolds for all possible $x_1^0 \in \mathbb{R}^{k_1}$ fill the whole of the phase space $\mathbb{R}^{k_1+k_2}$. This k_1-parametric family of nonintersecting k_2-dimensional manifolds filling the whole $k_1 + k_2$-dimensional space is called the *fast foliation* of that space, because it describes evolution of the system on the fast time scale. Each of the manifolds $x_1 = x_1^0$ makes a *leaf* of the fast foliation.

The slow-time system at $\epsilon = 0$ becomes

$$\frac{\mathrm{d}x_1}{\mathrm{d}t} = f_1(x_1, x_2), \tag{9}$$

$$0 = f_2(x_1, x_2), \tag{10}$$

i.e. a system of differential equations (9) with finite constraints (10). The finite constraints define a k_1-dimensional manifold in the $k_1 + k_2$ dimensional phase space, which is called the *slow manifold*. This also defines the fast variables x_2 as implicit functions of the slow variables, $x_2 = X(x_1)$, which reduces the original system of $k_1 + k_2$ equations to the k_1 equations on the slow manifold, which can be written in the form

$$\frac{\mathrm{d}x_1}{\mathrm{d}t} = f_1(x_1, X(x_1)). \tag{11}$$

If explicit solution of (10) in the form $x_2 = X(x_1)$ is possible, i.e. if the slow variables x_1 can be chosen as coordinates on the slow manifold, the procedure is often called an *adiabatic elimination* of the fast variables x_2. Otherwise, the procedure still can be used, but another system of coordinates on the slow manifold is required.

The classical Tikhonov (1952) theorem states exact conditions when a typical solution of the exact system starts with initial conditions at a point (x_1^0, x_2^0) demonstrates a "regular" behaviour, which consists of two parts. The first part of a regular solution is a transient period lasting for the time interval $t \propto \epsilon$ or $T \propto 1$, close to the solution of (8) within the leaf $x_1 = x_1^0$ starting from (x_1^0, x_2^0) and approaching the point $(x_1^0, X(x_1^0))$. The second part is slow motion along the slow manifold, it runs on the time scale $t \propto 1$ or $T \propto \epsilon^{-1}$ and the solution remains close to the solution of (11) with $x_2 = X(x_1)$ with initial conditions $(x_1^0, X(x_1^0))$. Apart from the technical conditions, the essential assumptions for this regular behaviour are that the slow manifold part of the trajectory consists of equilibria of the fast subsystem (8) which are stable (attractive) in linear approximation, and that the initial point (x_1^0, x_2^0) is within the basin of attraction of the equilibrium $(x_1^0, X(x_1^0))$ in terms of the fast subsystem (8).

If the trajectory along the slow manifold reaches a region where the points of the slow manifold no longer are stable equilibria of the fast subsystem, then usually it will take off away from the slow manifold, and there will be another fast piece of trajectory along the fast foliation. If the trajectory then happens to be in the basin of another stable part of the slow manifold, then, by Tikhonov's theorem, it will again have a quick transient along the fast foliation with subsequent slow motion along the slow manifold. The exact moment when a trajectory takes off from the slow manifold may depend on the initial conditions in a nontrivial way. Some trajectories may continue to go along the unstable part of the slow manifold for some time before taking off (so called "canard" or "French duck" solutions); in some systems such trajectories may even form the majority (Guckenheimer & Ilyashenko 2001). For the purposes of this paper, we ignore this difficulty, and assume that most trajectories take off as soon as they reach the border between the stable and the unstable regions of the slow manifold, and neglect the minority that do otherwise.

Tikhonov also presented a generalisation of the reduction theorem, for hierarchical systems that depend on more than one small parameter, for instance,

$$\begin{aligned}
\frac{\mathrm{d}x_1}{\mathrm{d}t} &= f_1(x_1, x_2, x_3), \qquad x_1 \in \mathbb{R}^{k_1}, \\
\epsilon_1 \frac{\mathrm{d}x_2}{\mathrm{d}t} &= f_2(x_1, x_2, x_3), \qquad x_2 \in \mathbb{R}^{k_2}, \\
\epsilon_1\epsilon_2 \frac{\mathrm{d}x_3}{\mathrm{d}t} &= f_3(x_1, x_2, x_3), \qquad x_3 \in \mathbb{R}^{k_3},
\end{aligned} \tag{12}$$

where simultaneously $\epsilon_1 \to +0$ and $\epsilon_2 \to +0$. In this case, a typical trajectory would consist of

1. a superfast part when only x_3 change while x_1 and x_2 remain constant during time $t \propto \epsilon_1^{-1}\epsilon_2^{-1}$, followed by

2. a fast part when x_3 and x_2 change, so that $f_3(x_1, x_2, x_3) \approx 0$, while x_1 remain constant, lasting $t \propto \epsilon_1^{-1}$, followed by

3. slow motion when all three sets of variables change with $f_3(x_1, x_2, x_3) \approx 0$ and $f_2(x_1, x_2, x_3) \approx 0$, on the time scale $t \propto 1$.

We will say that system (3,4) has *asymptotic structure* (k_1, k_2), and system (12) has asymptotic structure (k_1, k_2, k_3).

4 Zeeman's Examples

Zeeman (1972) has considered two "toy" models, demonstrating two different types of asymptotic behaviour of the shape of the action potential, which he believed resembled the shapes of the action potentials in nerve and in cardiac tissue. Thus, he called them the "Nerve" example and the "Heart" example. Without discussing how much these models actually relate to nerve or heart tissue, we briefly discuss them here, for the sake of introducing the key concepts and describing the method that we will subsequently apply to the HH system.

Zeemans analysis was purely phenomenological and based on the following qualitative observations on the biological excitable systems:

1. The system has a unique globally attracting equilibrium, called the **resting state**. Trajectories starting not too far from it, reach it remaining in its vicinity.

2. An external perturbation above a certain **threshold** can trigger an **"action"**. This means that trajectories starting further from the equilibrium than a locus in the phase space corresponding to the threshold, move *far away* from the equilibrium, at least for some time, before returning to the equilibrium. An initial piece of such a trajectory is characterised by a very fast, **"jump"** movement, compared to the typical overall time of the action. The subsequent slow motion of the system before returning back to the resting state, is called **excitation phase**, and the rapid motion before it after the superthreshold perturbation is called the **onset** of excitation.

3. The action trajectories eventually return to the equilibrium, but this return can be of two different types:

   (a) **Jump return**, including a significant piece of trajectory with a speed comparable to that of the onset jump. This is the behaviour in the "heart" model.

   (b) **Smooth return**, when the evolution remains as slow as during the excitation phase. This is the behaviour in the "nerve" model.

The quantity most easily observed in experiments is the transmembrane electric potential difference. The dependence of this potential difference on time for an "action" trajectory is called an **action potential**.

We remark here that in reality, the situation is often intermediate between cases 3a and 3b.

Zeeman's examples are in the form of a Tikhonov fast-slow system, so that the jump pieces of the action potential were along the fast foliation, and the smooth pieces were along the slow manifold.

4.1 The "Heart" example

Obviously, the stable equilibrium corresponding to the resting state must lie on the slow manifold. The threshold behaviour implies that in the leaf corresponding to the resting state, this state is not the only equilibrium, but there is at least one other equilibrium, corresponding to the excited state

(**bistability**). Then the threshold corresponds to the boundary between the basins of attraction of the two equilibria. The smooth part of the action potential can correspond to the movement along the slow manifold. The flow on the slow manifold has only one fixed point corresponding to the resting state.

To implement this situation, one fast variable and one slow variable are sufficient, i.e. it can be done in a system with asymptotic structure $(1,1)$. Zeeman proves that by presenting a concrete example:

$$\dot{b} = x - x_0, \tag{13}$$
$$\epsilon\dot{x} = -(x^3 - x + b), \tag{14}$$

where x is the fast variable and b is the slow variable. This example is very similar to the famous system of equations due to FitzHugh (1961).

The slow manifold is found by putting $\epsilon = 0$ in the $\dot{x}$ equation, which gives

$$f(x,b) = x^3 - x + b = 0.$$

The slow variable b cannot be chosen as a coordinate on this slow manifold, as this equation cannot be resolved with respect to the fast variable x. But it can be easily resolved with respect to b, and so x can be used as a coordinate.

The stable (attracting) regions on the slow manifold are defined by an additional condition that $\partial f/\partial x > 0$ and the unstable (repelling) region corresponds to $\partial f/\partial x < 0$. The boundary between these two regions satisfies the system of equations

$$f(x,b) = 0,$$
$$\frac{\partial f}{\partial x}(x,b) = 0,$$

which gives two solutions, $(x_1,b_1) = (1/\sqrt{3}, 2/3\sqrt{3})$ and $(x_2,b_2) = (-1/\sqrt{3}, -2/3\sqrt{3})$. These are the points at which trajectories moving along the slow manifold would take off from it.

The fast foliation. Since we have only one fast variable, the fast foliation is a family of lines $b = \text{const}$. The movement along the leaves is towards x-positive when $f < 0$ and towards x-negative when $f > 0$. In the leaves with $b \in (b_1, b_2)$ the fast subsystem has three equilibria, two of which are stable. Thus these two points are singular points of the projection of the slow manifold onto the b axis along the fast foliation.

The phase portrait resulting from the above analysis is shown on Figure 2(a). Points T' and T are the threshold/fold points (x_1,b_1) and (x_2,b_2). Letters M and M' label the attracting branches of the slow manifold, defined by $x^3 - x + b = 0$ and $3x^2 > 1$, and M" labels the repelling branch of the slow manifold, defined by $x^3 - x + b = 0$ and $3x^2 < 1$. The fixed point of the flow on the slow manifold is located on the attracting branch and therefore is stable. Trajectories starting at various points in the phase plane travel along the fast foliation to either of the pieces of slow manifold. Trajectories reaching the lower branch of the slow manifold, travel along it leftwards until reaching T' and cannot go any further as they have reached a piece of the slow manifold that is a repellor. Therefore such a trajectory has to make a jump from T' to the point A on the upper branch of the slow manifold, and then carry back along it to the stable equilibrium point. Trajectory BA'T'AE represents a typical action potential. The BA' part correspond to the jump onset. The A'T' represent the slow excitation part. The T'A piece is the jump return, and AE is the smooth part of the return to the equilibrium. The corresponding action potential is shown on Figure 2(b). Thus the Heart example demonstrates properties 1, 2 and 3a.

This example appears to be typical for systems with asymptotic structure $(1+1)$. One of the first results of the catastrophe theory (Zeeman 1977, pp. 497–561) is that the fold singularity is the only typical singularity that a one-parametric family of functions may have. Thus, the threshold behaviour and fast onset imply existence of two disjoint branches of the slow manifold and the necessity of a jump, rather than smooth, return. This leads to Zeeman's

Lemma 1 *In $\mathbb{R}^2$ a smooth return is not possible.*

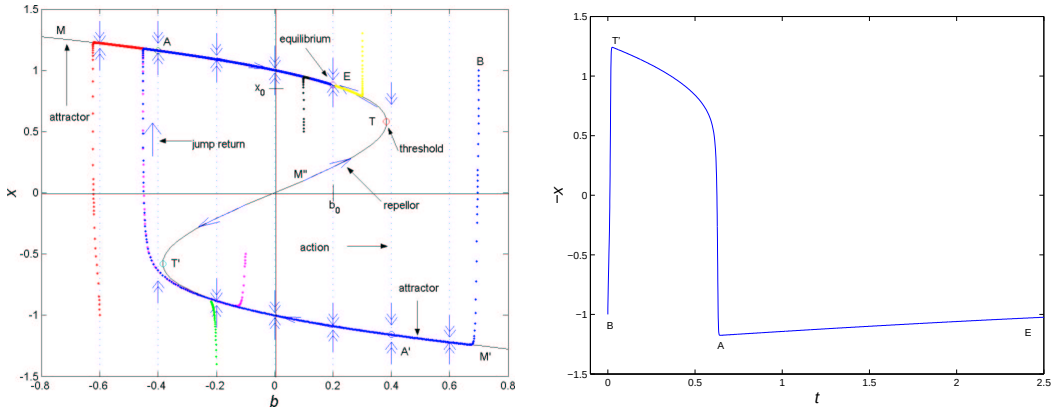

(a) (b)

Figure 2: Solutions of Zeeman's Heart example for $\epsilon = 1/200$. (a) Phase portrait. The double arrows represent the flow on the fast foliation and the single arrows represent the flow on the slow manifold. In this case the slow manifold is the line $b = -x^3 + x$. Dotted lines represent a selection of trajectories, distance between dots larger for faster motion. (b) "Action potential" corresponding to the blue trajectory of panel (a) with the initial point $(b, x) = (0.7, 1)$. Here the "voltage" is $-x$.

4.2 The "Nerve" example

The next result of the classical catastrophe theory is that in generic two-parametric families of functions, a new type of singularity is possible, the **cusp catastrophe**. The second Zeeman's toy model exploits this singularity to demonstrate a smooth return. It has the form of a $(2, 1)$ system:

$$\dot{a} = -2(a + x), \tag{15}$$
$$\dot{b} = -(a + 1), \tag{16}$$
$$\epsilon\dot{x} = -(x^3 + ax + b), \tag{17}$$

where a and b are the slow variables and x is the fast variable. The slow manifold is defined by the equation

$$f(x, a, b) = x^3 + ax + b = 0, \tag{18}$$

and the fast foliation is a 2-parametric family of lines $a = \text{const}$, $b = \text{const}$. The **bistability** is observed for those a and b for which (18) has three real solutions for x; the set of such a and b is defined by condition $27b^2 - 4a^3 > 0$. On the contrary, if $27b^2 - 4a^3 < 0$, then (18) has one simple real solution for x, and we call this the **monostability** region on the (a, b) plane. The boundary between these regions in the (a, b) plane is the semi-cubic parabola

$$27b^2 - 4a^3 = 0 \tag{19}$$

which corresponds to one triple (point $(0, 0)$) or one double and one simple (all other points) roots in (18).

Curve (19) is the projection onto the (a, b)-plane of the **fold curve**, defined as the set of points where the slow manifold is tangent to the fast foliation, $(0, 0, 1) \cdot \nabla f(a, b, x) = \partial f/\partial x = 0$. So the fold curves satisfies these two equations:

$$f(a, b, x) = 0 : \quad x^3 + ax + b = 0,$$
$$\frac{\partial f}{\partial x}(a, b, x) = 0 : \quad 3x^2 + a = 0,$$

and can be parameterised by x,

$$a = -3x^2,$$
$$b = 2x^3.$$

This is a smooth curve in the (a, b, x) space. Its projection to (a, b) plane is also a smooth curve except where it is tangent to the direction of the projection, i.e. to the fast foliation. Such tangency is characterised to the third condition

$$\frac{\partial^2 f}{\partial x^2}(a, b, x) = 0 : \qquad 6x = 0.$$

Thus, the only point where this tangency happens in this model is the point $(0, 0, 0)$ where equation (18) has a triple zero in x. This is the **cusp point** of the slow manifold.

The fold curve separates the stable (attracting) and unstable (repelling) regions of the slow manifold. Unlike the Heart example, where the fold points have cut the slow manifold onto three pieces, two stable and one unstable, here the fold curve only makes two pieces, one stable and one unstable. The unstable piece is projected onto the bistability region of the (a, b) plane, and corresponds to the middle zero x of the corresponding functions $f(x, a, b)$. The stable piece includes the monostability region together with the upper and lower branches of the manifold over the bistability region.

The **resting state** in this model is $(a, b, x) = (-1, 0, 1)$ and it belongs to the upper ("recovery") branch of the stable part of the manifold over the stability region. Thus we have the excitable behaviour: perturbation displacing the system from the resting state beyond the threshold, represented by the unstable branch of the slow manifold, fall down to the lower stable ("excitation") branch of the slow manifold, and return to the resting state from there. Unlike the Heart example, now there are two opportunities. Either a trajectory will reach the fold line and make a jump return to the upper branch of the slow manifold moving towards the resting state, or it can reach that state moving entirely within the slow manifold, by going around the cusp point, as now the upper and lower branches are connected to each other via the monostable region.

It is not possible to determine analytically, which of the two possibilities is realised for a given trajectory. Thus, it has to be done numerically. The **phase portrait**, showing the slow manifold, the fold line, and a selection of trajectories and a corresponding action potential on Figure 3.

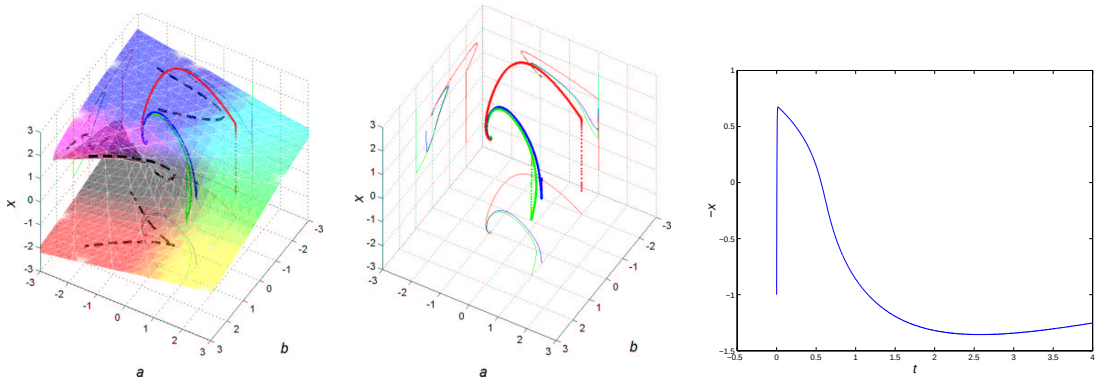

(a) (b) (c)

Figure 3: Phase Portrait of The Zeeman's Nerve example. The coloured semi-transparent surface is the slow manifold $x^3 + ax + b = 0$. The thick colour lines are trajectories (ϵ=1/200), and thin colour lines are their projections on the walls of the coordinate box. The solid black line is the fold curve; the dashed black lines are its projections. (a) The slow manifold, trajectories and the fold curve, with their projections. (b) The trajectories with their projections, but without the slow manifold and the fold curve. (c) Action potential ("voltage" $-x$ vs. time), corresponding to the blue trajectory of (a) and (b).

We can see that in this case, the action potential trajectory chooses the second option: it returns to the resting state entirely within the slow manifold, by going around the cusp point, from the excitation branch through the monostable region to the recovery branch. The corresponding

action potential of this "nerve" model demonstrates a jump onset of excitation, but a smooth return to equilibrium.

Thus, the "Nerve" example demonstrates properties 1, 2 and 3b.

5 Parametric embedding

We are going to apply the asymptotic procedure described above to the Hodgkin-Huxley system of equations (1,2). The immediate problem is that any asymptotic procedure, strictly speaking, applies not to a given system of equations, but to a family of systems depending on at least one parameter, to allow the limit when this parameter tends to zero or to infinity. However, the system of equations defined by (1,2) does not depend on any parameters, but only contains constants, which have been measured experimentally and have certain values, even if not always known with a good precision. Of course, we might consider physiologically feasible variations of the experiment, such as change of the ambient temperature (as indeed was done in the original paper by Hodgkin & Huxley (1952)), or ionic contents of the intracellular or extracellular solutions, so that some of the constants of (1) become parameters, which can vary from one experiment to another. However, this only provides parameters that can vary in certain finite ranges, and none of them can be reasonably assumed tending to zero or to infinity.

Thus, to apply the singular perturbation technique to our problem we need to introduce the small parameters artificially. This is of course a standard practice in principle, but the particular way we do it in this paper will be not quite usual, so we are going to formalise this procedure, to avoid confusion.

Definition We will call a system

$$\dot{x} = F(x;\epsilon), \qquad x \in \mathbb{R}^d,$$

depending on parameter ϵ, a *1-parametric embedding* of a system

$$\dot{x} = f(x), \qquad x \in \mathbb{R}^d,$$

if $f(x) \equiv F(x,1)$ for all $x \in \mathbb{R}^d$. Similarly, we define an *n-parametric embedding*, with right-hand sides in the form $F(x,\epsilon_1,\ldots,\epsilon_n)$ and $F(x,1,\ldots,1) \equiv f(x)$. If an n-parametric embedding has a form of a Tikhonov's fast-slow system with asymptotic structure $(k_1,\ldots,k_n)$, we call it a *(Tikhonov) $(k_1,\ldots,k_n)$-asymptotic embedding.*

The typical use of this procedure has the form of a replacement of a small constant with a small parameter. If a system contains a dimensionless constant a which is "much smaller than 1", then replacement of a with ϵa constitutes a 1-parametric embedding; and then the limit $\epsilon \to 0$ can be considered. In practice, constant a would more often be replaced with parameter ϵ, but in the context of the limit $\epsilon \to 0$ this, of course, does not make any difference from ϵa.

There are infinitely many ways a given system can be parametrically embedded. In terms of asymptotics, which of the embeddings is "better" is to some extent a matter of taste, but in any case depends on the qualitative features of the original systems that need to be represented, or classes of solutions that need to be approximated by the embedding taken to the limit. If a numerical simulation of the interesting properties can be done easily, then the practical recipe which we use in this paper, is to look at the solution of the embedding at different, progressively decreasing values of the artificial small parameter ϵ, and see when the features of interest will start to converge. If the convergent behaviour is satisfactorily similar to the original system with $\epsilon = 1$, the embedding is adequate for these features.

6 A $(2,1,1)$-asymptotic embedding of the Hodgkin-Huxley system

6.1 Standard values of the parameters

As follows from above, before proceeding with the asymptotic analysis of the HH system, we need to do an asymptotic embedding. To do that, we need to decide what features the singularly perturbed system should represent. In this paper, we are most interested in the shape of the action potential, i.e. a typical trajectory that starts not too far from the resting state equilibrium but returns to it after performing a relatively long excursion in the phase space. A helpful feature of the HH system is that it has a quasi-linear form, where each equation is linear with respect to its "own" variable, but the coefficients of that linear dependence depend on other variables:

$$\begin{aligned}
\frac{\mathrm{d}E}{\mathrm{d}t} &= \frac{\overline{E}(h,m,n)-E}{\tau_E(h,m,n)},\\
\frac{\mathrm{d}h}{\mathrm{d}t} &= \frac{\overline{h}(E)-h}{\tau_h(E)},\\
\frac{\mathrm{d}m}{\mathrm{d}t} &= \frac{\overline{m}(E)-m}{\tau_m(E)},\\
\frac{\mathrm{d}n}{\mathrm{d}t} &= \frac{\overline{n}(E)-n}{\tau_n(E)},
\end{aligned}$$

where,

$$\begin{aligned}
\overline{E}(h,m,n) &= \frac{\overline{g}_{Na}m^3hE_{Na}+\overline{g}_K n^4E_K+\overline{g}_l E_l}{\overline{g}_{Na}m^3h+\overline{g}_K n^4+\overline{g}_l},\\
\tau_E(h,m,n) &= \left(\overline{g}_{Na}m^3h+\overline{g}_K n^4+\overline{g}_l\right)^{-1}.
\end{aligned}$$

Now we consider an action potential solution, E, n, m and h as functions of t. Then we have all τ's as functions of t, via $\tau_j(t)=\tau(j(t))$, where $j=E,h,m,n$. Speaking informally, these τ's represent the "fastness" of each of the dynamic variables, and as it changes in the course of the action potential. The graph of these functions in semi-logarithmic coordinates is shown on Figure 4.

We can see that variables E and m are always faster than variables h and n, and that compared to each other, m is slower than E in the beginning of the action potential, but faster than E in the most part of the action potential. That means, that the most correct asymptotic embedding of this system would be $(2,2)$, with two slow (h,n) and two fast (E,m) variables. Such embedding will be analysed in the next section; in this section, however, we start from a $(2,1,1)$ embedding, considering E as a fast and m as a superfast variable. This means, we first project the dynamics to the slow manifold with respect to m ("adiabatically eliminate" this variable), which will give us a system of three equations. Then we analyse this system of three equations as a $(2,1)$ Tikhonov system, using the same asymptotic and visualisation techniques as in Zeeman's Nerve example. The reasons for doing this approach are that

- the adiabatic elimination of m is often done in numerical computations of detailed models of cardiac equations, so it is worth considering how well justified is this approach on a concrete example,
- analysis of a three-dimensional system is easier for understanding, as three-dimensional graphics can be used, which is not possible for four-dimensional systems, and
- as we shall eventually see, the results of the $(2,2)$ embedding in this case actually coincide with the results of the $(2,1,1)$ embedding.

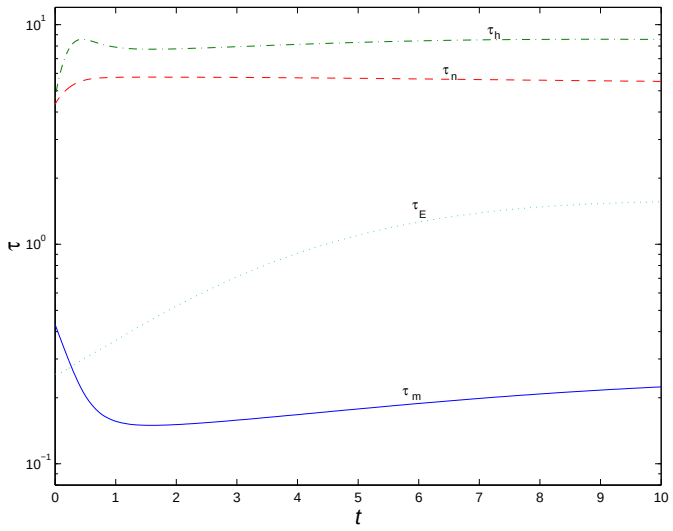

Figure 4: Characteristic times of the dynamic variables, as they change during the action potential shown on Figure 1.

Thus, we consider the following two-parametric embedding of (1):

$$\begin{aligned}
\frac{\mathrm{d}n}{\mathrm{d}t} &= \frac{(\overline{n}-n)}{\tau_n}, \\
\frac{\mathrm{d}h}{\mathrm{d}t} &= \frac{(\overline{h}-h)}{\tau_h}, \\
\epsilon_1 \frac{\mathrm{d}E}{\mathrm{d}t} &= -C_M^{-1}\left(\overline{g}_K n^4 (E-E_K) + \overline{g}_{Na} m^3 h (E-E_{Na}) + \overline{g}_l (E-E_l)\right), \\
\epsilon_1\epsilon_2 \frac{\mathrm{d}m}{\mathrm{d}t} &= \frac{(\overline{m}-m)}{\tau_m},
\end{aligned} \tag{20}$$

with artificial small parameters ϵ_1 and ϵ_2.

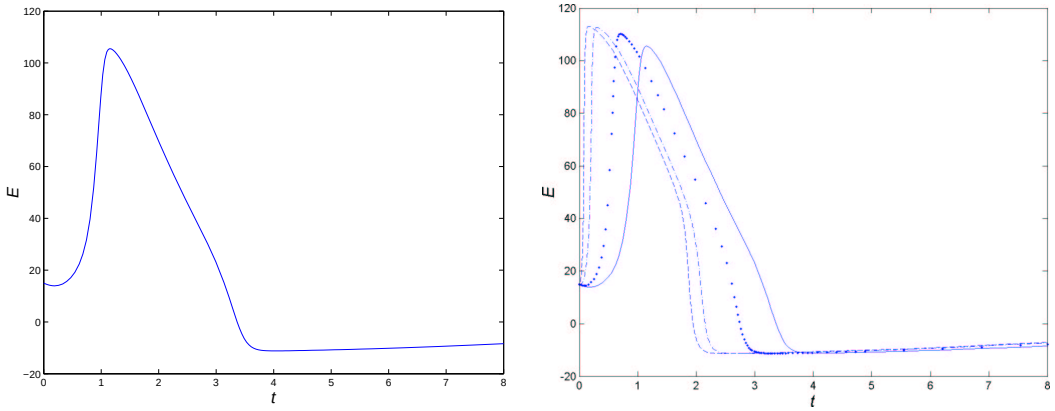

(a) (b)

Figure 5: The first asymptotic embedding. (a) The action potential in the full system (1), equivalently (20) with $\epsilon_1 = \epsilon_2 = 1$. Initial conditions $E(0) = 15$, $m(0) = 0.0530$, $h(0) = 0.5961$, $n(0) = 0.3177$. (b) The action potentials in (20) at the same initial conditions with $\epsilon_1 = 1$ and progressively decreasing values of ϵ_2: 1, 0.5, 0.1 and 0.01.

First we consider the limit $\epsilon_2 \to +0$. The effect of this limit onto the shape of the action

potential is shown on Figure 5. We can see that while the excitability of the model is preserved, and we still observe Zeeman's properties 1 and 2, i.e. the resting state and jump upstroke to the excited state, the asymptotic embedding changes the property 3b, the smooth return to rest, to 3a, the jump return to rest.

The corresponding slow manifold is defined by equating the right-hand side of the last equation to zero, which gives m as a single-valued smooth function of E,

$$m = \overline{m}(E). \tag{21}$$

In other words, the slow manifold of the superfast limit, being a three-dimensional manifold in the four-dimensional phase hyperspace (n, h, E, m), is uniquely and smoothly projected onto the three-dimensional reduced phase space (n, h, E). The equations on this slow manifold can be defined by equations in this phase space. These make a $(2, 1)$ Tikhonov system

$$\begin{aligned}
\frac{\mathrm{d}n}{\mathrm{d}t} &= \frac{(\overline{n} - n)}{\tau_n}, \\
\frac{\mathrm{d}h}{\mathrm{d}t} &= \frac{(\overline{h} - h)}{\tau_h}, \\
\epsilon_1 \frac{\mathrm{d}E}{\mathrm{d}t} &= f_E(h, n, E) = C_M^{-1} \left[\overline{g}_{Na}(E_{Na} - E) h \overline{m}^3(E) + \overline{g}_K(E_K - E) n^4 + \overline{g}_l(E_l - E) \right].
\end{aligned} \tag{22}$$

The slow manifold of (22) is given by

$$f_E(h, n, E) = 0. \tag{23}$$

This equation can not be explicitly resolved with respect to E, but is easily resolved with respect to h, giving

$$h = -\frac{\overline{g}_K(E_K - E) n^4 + \overline{g}_l(E_l - E)}{\overline{g}_{Na}(E_{Na} - E)\overline{m}^3(E)}. \tag{24}$$

This feature is similar to Zeeman's Nerve example: the slow manifold equation is not uniquely solvable for the fast variable, but is uniquely solvable for one of the slow variables. This explicit representation of the slow manifold is convenient for visualisation.

Since there is only one fast variable now, the fast foliation consists of all lines $h = \text{const}$ and $n = \text{const}$. The dynamics on a fast leaf with given h and n is determined by one differential equation

$$\frac{\mathrm{d}E}{\mathrm{d}T} = f_E(h, n, E), \tag{25}$$

where $T = t/\epsilon$ is the fast time. Thus, the qualitative dynamics on a fast leaf is fully determined by the equilbria on it, i.e. the points where that leaf crosses the slow manifold. A numerical analysis of the dependence of the right-hand side of the fast equation on E shows that for different h and n, a leaf may have from one (monostable) to three (bistable) intersections. This is different from the previous reduction by the superfast variable m where there was always one intersection, and quite similar to Zeeman's Nerve example.

As in the Nerve example, we shall describe the monostable and bistable regions via the boundary between them. On that boundary, function f_E as a function of E has a repeated root. Geometrically, this means that this boundary is a projection onto the (h, n) plane of the **fold curve** in the (h, n, E) space, defined as the set of points where the slow manifold is tangent to the direction of the fast foliation, $(0, 0, 1)$. This means that the curve is a solution of a system of two finite equations,

$$f_E(h, n, E) = 0: \quad \overline{g}_K(E_K - E) n^4 + \overline{g}_{Na}(E_{Na} - E) h \overline{m}^3(E) + \overline{g}_l(E_l - E) = 0, \tag{26}$$

$$\frac{\partial f_E}{\partial E}(h, n, E) = 0: \quad -\overline{g}_K n^4 - \overline{g}_{Na} h \overline{m}^3(E) - \overline{g}_l + \overline{g}_{Na}(E_{Na} - E) h \left(\overline{m}^3(E)\right)' = 0. \tag{27}$$

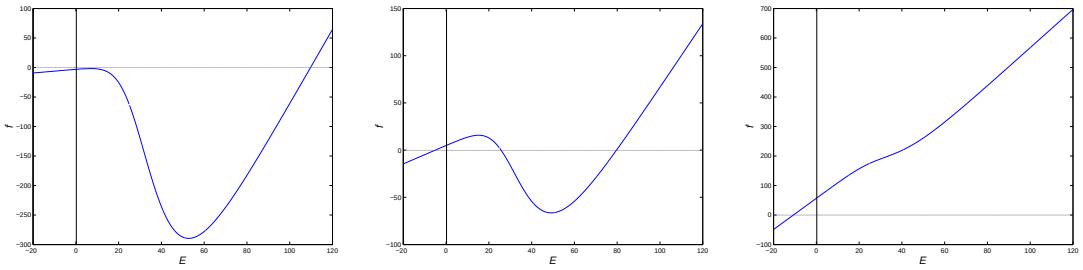

(a) (b) (c)

Figure 6: The dynamics $f_E(h, n, E)$ on the different fast leafs: (a) for $h = 0.05$, $n = 0.14$ (in the monostability region), (b) for $h = 0.02$, $n = 0.37$ (in the bistability region), (c) for $h = 0.01$, $n = 0.61$ (in the monostability region).

This implicit definition of the fold curve can be made explicit (parametric), by choosing E as a parameter. That means, resolving system (26,27) with respect to h and n, we get

$$h = \frac{\overline{g}_l}{\overline{g}_{Na}} \frac{(E_K - E_l)}{(E_{Na} - E_K)\overline{m}^3(E) + (E - E_{Na})(E - E_K)\left(\overline{m}^3(E)\right)'}, \tag{28}$$

$$n = \left(\frac{\overline{g}_l}{\overline{g}_K} N(E)\right)^{1/4}, \tag{29}$$

where

$$N(E) = \frac{(E_{Na} - E_l)\overline{m}^3(E) + (E - E_{Na})(E - E_l)\left(\overline{m}^3(E)\right)'}{(E_K - E_{Na})\overline{m}^3(E) - (E - E_{Na})(E - E_K)\left(\overline{m}^3(E)\right)'} = -\frac{q_1(E) - \mu(E)}{q_2(E) - \mu(E)}, \tag{30}$$

and

$$\begin{aligned} \mu(E) &= \overline{m}(E)/\left(3\overline{m}'(E)\right), \\ q_1(E) &= (E_{Na} - E)(E - E_l)(E_{Na} - E_l)^{-1}, \\ q_2(E) &= (E_{Na} - E)(E - E_K)(E_{Na} - E_K)^{-1}. \end{aligned} \tag{31}$$

As n must be real, equation (29) only makes sense when $N(E) > 0$. The graph of functions $N(E)$, $\mu(E)$ and $q_{1,2}(E)$ for the standard values of the parameters is shown on Figure 7. There are two disjoint intervals, $E \in [-9.37\ldots, 14.66\ldots]$ and $E \in [41.25\ldots, 45.68\ldots]$, where it is positive. Thus, the fold curve consists of two disjoint branches.

The cusp point is, as in Zeeman's Nerve example, defined by condition that $f(h, n, E)$ has a triple zero on E, or, equivalently, that the fold curve is tangent to the direction of the fast foliation $(0, 0, 1)$. This means that in addition to the two equations (26,27), the cusp point satisfies also

$$\frac{\partial^2 f}{\partial E^2}(h, n, E) = 0: \qquad \overline{g}_{Na} h M''(E) = 0, \text{ where } M(E) = (E - E_{Na})\overline{m}^3(E). \tag{32}$$

Thus the E-coordinate of the cusp points, if any, is given by the inflexion points of the graph of the function $M(E)$. For the standard parameter values, there is only one such point, $E_* \approx 31.9$. The value of $N(E)$ at this point is negative, $N(E_*) \approx -0.021$. Therefore, the slow manifold at the standard parameter values does not have cusp points.

The phase portrait resulting from the above analysis is shown on Figure 8. In panel (a), we can see the slow manifold as the surface, the fold curve and its projections as black lines and the trajectories and their projections as colour lines. We use (24) to draw the slow manifold, and (28,29) to draw the fold curve. This can be seen by the thick black broken line in figure 8(a). The equilibrium values of n and h were used as initial points for the trajectories, with E displaced from its equilibrium value 0 mV by different amounts.

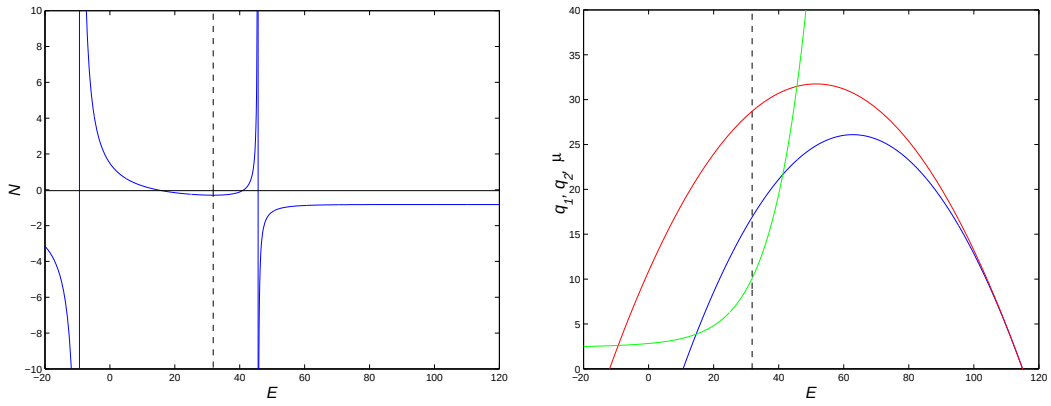

(a) (b)

Figure 7: (a) Function $N(E)$ defined by (30), for the standard parameter values. (b) Functions $q_1(E)$ (blue), $q_2(E)$ (red) and $\mu(E)$ (green) defined by (31). Vertical dashed line is $E = E_* \approx 31.9$.

Figure 8(a) also shows a typical trajectory that goes from its starting point along the fast foliation until it reaches the slow manifold, then along the slow manifold, possibly until the fold curve, where we have a jump return down the fast foliation to the slow manifold. Every trajectory eventually moves to the equilibrium point $(h, n, E) = (0.5961, 0.3177, 0)$.

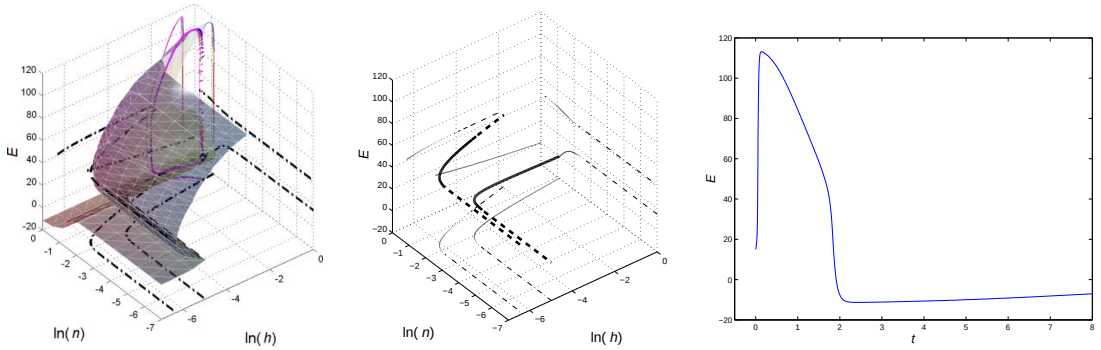

(a) (b) (c)

Figure 8: (a) The phase portrait of the reduced system (22), for the standard values of the parameters. The coloured semi-transparent surface is the slow manifold (23). The solid black line is the fold curve; the dashed black lines are its projections. The trajectories and their projections are in the other colours. The initial points of the trajectories are at n=0.3177 and h=0.5961, and $E = 6\,\text{mV}$ (magenta), $7\,\text{mV}$ (green), $15\,\text{mV}$ (red) and $90\,\text{mV}$ (blue). The black circle is the equilibrium point $n = 0.3177$, $h = 0.5961$ and $E = 0\,\text{mV}$. (b) Same as (a), but only the fold curve (the bold line) and its projections on the (n, h), (E, n) and (E, h) plane. The fold curve consists of two disjoint branches; there is no cusp point. (c) The action potential corresponding to the red trajectory of (a) and (b).

6.2 Variation of parameters can produce a cusp

We now demonstrate that a variation of parameters in the HH system is possible that gives $N(E_*) > 0$, so the slow manifold has a real cusp point. From (30) we can see that the sign of $N(E_*)$ depends on the relative location of the roots of the equations $q_{1,2}(E) - \mu(E)$ to E_*. Note that the function $\mu(E)$ is determined by the properties of the activation gates of the Na channel, and variations of those are not physiologically plausible. On the contrary, the parameters E_{Na}, E_K and

E_l are determined by the ratios of the intra- and extracellular concentrations of the corresponding ions, which can be changed during the experiments, and can vary physiologically depending on the ionic balance of the organism. From Figure 7(b) one can see that the closest to the E_* root of $q_{1,2}(E) = \mu(E)$ is the left root of $q_1(E)$, obviously strongly depending on E_l. Incidentally, as we noted above, E_l is the least reliable parameter of the model. We have found that by changing E_l from its standard value of 10.613, we can shift the left zero of $q_1(E) - \mu(E)$ through $E_* = 31.9$. Notably, this parameter variation does not involve function $M(E)$ whose inflexion point is E_*, so the value of E_* remains unchanged. As a result, at $E_l = 21$ and all other parameters at standard values, we have $N(E_*) = 0.00017$, and there is a cusp point, $(h, n, E) = (0.0012, 0.114, 31.9)$.

The Phase Portrait of the (2,1) system with $E_l = 21$ is shown on Figure 9. Notations are the same as in Figure 8, plus the cusp point is shown as a red star.

We can see from this phase portrait that excitable properties in this modified HH system remain the same as in the original system. As before, a typical action trajectory moves from its initial point along the fast foliation, parallel to the E axis, until it reaches the slow manifold. Then it travels down the slow manifold until the fold curve, where it takes off from the slow manifold, along the fast foliation again to another branch of the slow manifold, and then along it to the equilibrium point which is now at (h, n, E)=$(0.5961, 0.40, 0)$. Thus, although the slow manifold now has a cusp point, an action trajectory does not go around it, and has a jump return.

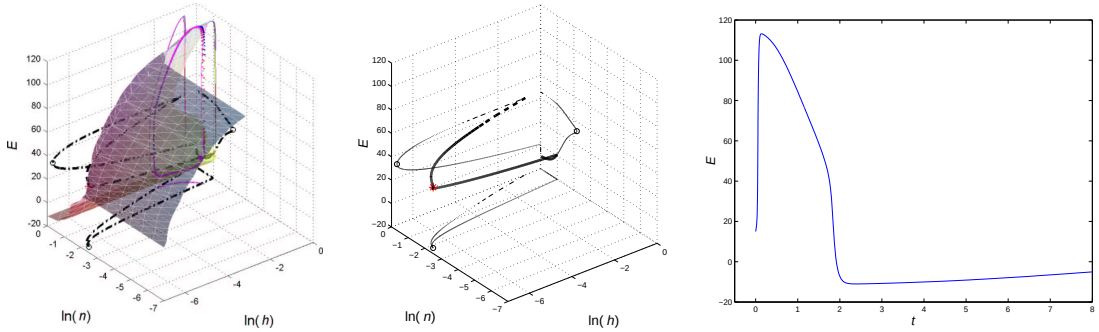

(a) (b) (c)

Figure 9: (a) Phase portrait of the system (22) with $E_l = 21$. The slow manifold is the surface; the fold curve and its projections are in black. The trajectories and their projections are in the other colours. The trajectories are at initial points $n = 0.3177$, $h = 0.5961$ and $E = 6$ (magenta), 7 (green) 15 (red), and 90 (blue) mV. The red star represents the cusp point (h, n, E)=$(0.0012, 0.114, 31.9)$. (b) Same as (a), but without the surface and the trajectories. The thin black lines are the projections on the (n, h), (E, n) and (E, h) plane of the fold curve (c) The action potential corresponding to the red trajectory of (a).

7 A $(2, 2)$-asymptotic embedding

Now we do the following parametric embedding of the HH system,

$$\begin{aligned}
\frac{\mathrm{d}n}{\mathrm{d}t} &= \frac{(\overline{n} - n)}{\tau_n}, \\
\frac{\mathrm{d}h}{\mathrm{d}t} &= \frac{(\overline{h} - h)}{\tau_h}, \\
\epsilon\frac{\mathrm{d}E}{\mathrm{d}t} &= -C_M^{-1}\left(\overline{g}_K n^4(E - E_K) + \overline{g}_{Na} m^3 h(E - E_{Na}) + \overline{g}_l(E - E_l)\right), \\
\epsilon\frac{\mathrm{d}m}{\mathrm{d}t} &= \frac{(\overline{m} - m)}{\tau_m}.
\end{aligned} \tag{33}$$

with one artificial small parameter ϵ. This embedding takes into account the real relationship between the characteristic time scales of dynamic variables during a typical action potential solution. This implies that E and m are considered as (in principle equally) fast variables, and n and h as slow variables.

The slow manifold is defined by equating the right hand sides of the two fast equations, that is,

$$\begin{aligned} &\phi(n,h,E,m) = \overline{g}_K n^4 (E - E_K) + \overline{g}_{Na} m^3 h (E - E_{Na}) + \overline{g}_l (E - E_l) = 0, \\ &m = \overline{m}(E). \end{aligned} \tag{34}$$

Since $\phi(n,h,E,\overline{m}(E)) \equiv f(n,h,E)$, this coincides with the slow manifold of the $(2,1,1)$ embedding, as expected. More accurately, the slow manifold (34) of the $(2,2)$ system (33), a two-dimensional manifold in the four-dimensional phase space $\mathbb{R}^4 = \{(n,h,m,E)\}$, is the lifting by (21) of the slow manifold (23) of the $(2,1)$ system (22), a two-dimensional manifold in the three-dimensional phase space $\mathbb{R}^3 = \{(n,h,E)\}$.

The fast foliation of (33) is a two-parametric set of the planes $n = \text{const}$, $h = \text{const}$ in $\mathbb{R}^4 = \{(n,h,m,E)\}$. The flow within each of these planes is described by system of two equations, which in the fast time T state

$$\begin{aligned} \frac{\mathrm{d}E}{\mathrm{d}T} &= -C_M^{-1} \phi(n,h,E,m), \\ \frac{\mathrm{d}m}{\mathrm{d}T} &= \frac{(\overline{m} - m)}{\tau_m}. \end{aligned} \tag{35}$$

Again, since $\phi(n,h,E,\overline{m}(E)) \equiv f(n,h,E)$, then the equilibria in (35) can be obtained by lifting of the equilibria in (25) by (21). In particular, the number of equilibria in (25) is the same as in (35), and we only need to establish their stability.

The Jacobian of the right-hand sides of (35) at an equilibrium is

$$J = \frac{\partial(\dot{E},\dot{m})}{\partial(E,h)} = \begin{bmatrix} -C_M^{-1}\partial\phi/\partial E & -C_M^{-1}\partial\phi/\partial m \\ (\tau_m \overline{m}' - (\overline{m} - m)\tau_m')\,\tau_m^{-2} & -\tau_m^{-1} \end{bmatrix}.$$

However, since at an equilibrium $m = \overline{m}(E)$, this reduces to

$$J = \begin{bmatrix} -C_M^{-1}\partial\phi/\partial E & -C_M^{-1}\partial\phi/\partial m \\ \overline{m}'\tau_m^{-1} & -\tau_m^{-1} \end{bmatrix}.$$

An equilibrium is stable in linear approximation iff $\mathrm{Tr}J < 0$ and $\det J > 0$. We have

$$\mathrm{Tr}J = -C_M^{-1}\frac{\partial\phi}{\partial E} - \tau_m^{-1} = -C_M^{-1}\left(\overline{g}_K n^4 + \overline{g}_{Na} m^3 h + \overline{g}_l\right) - \tau_m^{-1} < 0$$

for all physiologically sensible values of the variables, so the first stability condition is always satisfied. Further,

$$\det J = C_M^{-1}\tau_m^{-1}\left(\frac{\partial\phi}{\partial E} + \frac{\partial\phi}{\partial m}\frac{\mathrm{d}\overline{m}}{\mathrm{d}E}\right) = C_M^{-1}\tau_m^{-1}\frac{\partial f}{\partial E},$$

where $f(n,h,E) = \phi(n,h,E,\overline{m}(E))$ is the right hand side of the fast equation of the $(2,1)$ system (22). Thus, an equilibrium in the $(2,2)$ system (33) is stable if and only if the corresponding equilibrium in the $(2,1)$ system (22) is stable. In particular, **the fold curve**, i.e. the boundary between the attractive and repelling regions of the slow manifold, coincide in (22) and (33) up to the lifting (21). The formal condition of the fold curve is now $\det J = 0$.

Thus, we see that the results of this $(2,2)$ embedding coincide with the results of the $(2,1,1)$ embedding, with a possible exception of the exact character of the "jump" transients from one branch of the slow manifold to another.

8 Conclusion

We have analysed the asymptotic behaviour of the Hodgkin-Huxley system of equations, using its parametric embeddings that make it a Tikhonov fast-slow system. One particular goal was to check directly Zeeman's conjecture that the shape of the action potential in this system is related to the cusp catastrophe of the slow manifold in such an embedding.

The result of our analysis is that although the main property of excitability of the HH system survives this embedding, some qualitative changes happen to the action potential; in particular, the "smooth" return from excitation becomes a "jump" return. We have established this by numerical simulation of the embedding system, prior to any asymptotic analysis. Thus, this feature is not necessarily a consequence of the geometry of the slow manifold.

In fact, we have shown that the geometry of the slow manifold can vary qualitatively, within physiologically feasible variations of the parameters. Namely, it may or may not have a cusp singularity with respect to the fast foliation. At standard Hodgkin-Huxley parameter values, the slow manifold has two attracting regions of excitation and recovery, separated from each other and bordering the repelling threshold region by two disjoint fold curves. However, variation of the leakage current reversal potential can make the two attracting regions connected via an isthmus in the monostability region, so the attracting part of the slow manifold becomes a whole piece, separated from the threshold region by a single fold line, which has a projection onto the plane of slow variables with a return point. This, however, does not influence the shape of the action potential, as the typical action trajectories do not take the possibility of returning to the resting state along the slow manifold by going around the cusp point, but still return to it by jumping from the excitation to the recovery branch.

Thus, we conclude that Zeeman's conjecture has been partly confirmed: the slow manifold of the HH system can have a cusp singularity, but this does not affect the shape of the action potential, which in the Tikhonov limit remains similar to that of Zeeman's "Heart" example or FitzHugh's system (jump onset, jump return), rather than Zeeman's "Nerve" example (jump onset, slow return).

Equations of other biological excitability models are related to the Hodgkin-Huxley equations, and some of those equations, e.g. equations of excitation in heart, do present significant difference in speed of onset and return. The fact that the slow manifold in Hodgkin-Huxley system can have a cusp singularity, suggests that Zeeman's conjecture may be relevant to some of these systems.

On the other hand, this means that to explain properly the shape of the action potential in the HH system, and perhaps some other biological excitability models, one must go beyond Tikhonov perturbation theory, i.e. consider asymptotic embedding where the small parameters appear not as factors at some of the derivatives, but in some other ways. An example of such a non-Tikhonov embedding, relevant to a particular mechanism of excitation propagation block, is presented in (Biktashev 2002, Biktashev 2003).

Acknowledgements

VNB is grateful to D. Barkley and I.V. Biktasheva for encouraging discussions. This work was supported in part by EPSRC.

References

Bernus, O., Wilders, R., Zemlin, C. W., Verschelde, H. & Panfilov, A. V. (2002), 'A computationally efficient electrophysiological model of human ventricular cells', *Am. J. Physiol.* **282**, H2296–H2308.

Biktashev, V. N. (2002), 'Dissipation of excitation wavefronts', *Phys. Rev. Lett.* **89**(16). To appear.

Biktashev, V. N. (2003), 'A simplified model of propagation and dissipation of excitation fronts', *Int. J. of Bifurcation and Chaos* . Submitted (in this issue).

Duckett, G. & Barkley, D. (2000), 'Modeling the dynamics of cardiac action potentials', *Phys. Rev. Lett.* **85**, 884–887.

Elkin, Y. E., Biktashev, V. N. & Holden, A. V. (2002), 'Waves of constant shape and the structure of the "rotors boundary" in excitable media', *Chaos Solitons & Fractals* **14**, 385–395.

Fenton, F. & Karma, A. (1998), 'Vortex dynamics in three-dimensional continuous myocardium with fiber rotation: Filament instability and fibrillation', *Chaos* **8**, 20–47.

FitzHugh, R. (1961), 'Impulses and physiological states in theoretical models of nerve membrane', *Biophysical Journal* **1**, 445–456.

Guckenheimer, J. & Ilyashenko, Y. (2001), 'The duck and the devil: Canards on the staircase', *Moscow Mathematical Journal* **1**(1), 27–47.

Hinch, R. (2002), 'An analytical study of the physiology and pathology of the propagation of cardiac action potentials', *Progress in Biophysics and Molecular Biology* **78**, 45–81.

Hodgkin, A. L. & Huxley, A. F. (1952), 'A quantitive description of membrane current and it's application to conduction and excitation in nerve', *J. Physiol* **117**, 500–544.

Tikhonov, A. N. (1952), 'Systems of differential equations, containing small parameters at the derivatives', *Mat. Sbornik* **31**, 575–586.

Tyson, J. J. & Keener, J. P. (1988), 'Singular perturbation theory of traveling waves in excitable media (a review)', *Physica D* **32**, 327–361.

Zeeman, E. C. (1972), *Differential Equations For The Heartbeat And Nerve Impulse*, Mathematics Institute, University Of Warwick, Coventry.

Zeeman, E. C. (1977), *Catastrophe Theory. Selected papers 1972–1977*, Addison-Wesley, Reading, MA.